

**Semi-Active Control Algorithms for Structures with  
Variable Dampers**

---

---

Fahim Sadek and Bijan Mohraz

Building and Fire Research Laboratory  
Gaithersburg, Maryland 20899



**United States Department of Commerce  
Technology Administration  
National Institute of Standards and Technology**

# Semi-Active Control Algorithms for Structures with Variable Dampers

---

---

Fahim Sadek and Bijan Mohraz

October 1997  
Building and Fire Research Laboratory  
National Institute of Standards and Technology  
Gaithersburg, MD 20899



**U.S. Department of Commerce**  
William M. Daley, *Secretary*  
Technology Administration  
Gary R. Bachula, *Acting Under Secretary for Technology*  
National Institute of Standards and Technology  
Robert E. Hebner, *Acting Director*

## ABSTRACT

Semi-active control systems combine the features of active and passive control to reduce the response of structures to various dynamic loadings. They include: a) active variable stiffness where the stiffness of the structure is adjusted to establish a non-resonant condition between the structure and excitation, and b) active variable damper where the damping coefficient of the device is varied to achieve the most reduction in the response.

This study is concerned with examining the effectiveness of variable dampers for seismic applications. Three algorithms for selecting the damping coefficient of variable dampers are presented and compared. They include: a linear quadratic regulator (LQR) algorithm, a generalized LQR algorithm where a penalty is imposed on the acceleration response, and a displacement-acceleration domain algorithm where the damping coefficient is selected by examining the response on the displacement-acceleration plane and assigning different damping coefficients accordingly. Two single-degree-of-freedom structures subjected to 20 ground excitations are analyzed using the three algorithms. The analyses indicate that unlike passive dampers where for flexible structures, an increase in damping coefficient decreases the displacement but increases the acceleration response, variable dampers can be effective in reducing both the displacement and acceleration responses. The study indicates that the generalized LQR algorithm is more efficient than the other two in reducing the displacement and acceleration responses. The algorithms are used to compute the seismic response of two flexible structures -- an isolated bridge modeled as a single-degree-of-freedom system and a base-isolated six-story frame modeled as a multi-degree-of-freedom system. The results indicate that variable dampers reduce the displacement and acceleration responses of the two structures to a significant degree.

**Key Words:** Building technology; Control algorithms; Seismic design; Semi-active control; Structural dynamics; Variable dampers

**BLANK PAGE**

## **ACKNOWLEDGMENTS**

This study was supported by the Structures Division, Building and Fire Research Laboratory, National Institute of Standards and Technology, U.S. Department of Commerce through a grant to Southern Methodist University.

Dr. Sadek is a Post-doctoral Fellow at SMU and NIST; Dr. Mohraz is Professor of Mechanical Engineering at SMU, on an Intergovernmental Personnel Act assignment at NIST.

Suggestions made by Dr. Marek Franaszek, NIST and Dr. Timothy Whalen, Purdue University are gratefully acknowledged.

**BLANK PAGE**

## TABLE OF CONTENTS

ABSTRACT .....	iii
ACKNOWLEDGMENTS .....	v
TABLE OF CONTENTS .....	vii
LIST OF FIGURES .....	ix
LIST OF TABLES .....	xi
1. INTRODUCTION .....	1
2. SUMMARY OF PREVIOUS WORK .....	3
3. DISCUSSION AND ANALYSIS .....	5
4. SEMI-ACTIVE CONTROL ALGORITHMS .....	7
4.1 Semi-Active LQR Algorithm .....	7
4.2 Semi-Active Generalized LQR Algorithm .....	9
4.3 Semi-Active Displacement-Acceleration Domain Algorithm .....	14
4.4 Discussion and Comparison of Algorithms .....	17
5. APPLICATIONS .....	19
5.1 Bridge .....	19
5.2 Base-Isolated Frame .....	19
6. CONCLUSIONS .....	23
REFERENCES .....	25
APPENDIX A. EARTHQUAKE RECORDS USED IN THE STATISTICAL STUDY .....	27
APPENDIX B. LIST OF SYMBOLS .....	29

**BLANK PAGE**



## LIST OF FIGURES

Figure 4.1	Variation of the displacement and acceleration response ratios with $q$ for the SDOF structure with $T = 0.2$ s using algorithm SA-1 .....	10
Figure 4.2	Variation of the displacement and acceleration response ratios with $q$ for the SDOF structure with $T = 3.0$ s using algorithm SA-1 .....	10
Figure 4.3	Variation of the displacement and acceleration response ratios with $q_a$ for the SDOF structure with $T = 0.2$ s using algorithm SA-2 .....	13
Figure 4.4	Variation of the displacement and acceleration response ratios with $q_a$ for the SDOF structure with $T = 3.0$ s using algorithm SA-2 .....	13
Figure 4.5	Displacement-acceleration Domain for algorithm SA-3 .....	14
Figure 4.6	Variation of the displacement and acceleration response ratios with $\Omega$ for the SDOF structure with $T = 0.2$ s using algorithm SA-3 .....	16
Figure 4.7	Variation of the displacement and acceleration response ratios with $\Omega$ for the SDOF structure with $T = 3.0$ s using algorithm SA-3 .....	16

**BLANK PAGE**

## LIST OF TABLES

Table 3.1	Summary of the average response ratios for six SDOF structures with passive damping .....	6
Table 4.1	Summary of the average response ratios for the structure ( $T = 3.0$ s) with passive and semi-active dampers .....	9
Table 5.1	Summary of the response of the bridge with no control and with passive and semi-active dampers .....	21
Table 5.2	Response of the six-story base-isolated frame to the Pacoima Dam accelerogram .....	21
Table 5.3	Response of the six-story base-isolated frame to the Taft accelerogram .....	22

## 1. INTRODUCTION

New concepts for active and passive control have been developed for reducing the response of structures to wind, earthquake, blast, and other dynamic loadings. Passive control refers to systems that utilize the response of structures to develop the control forces without requiring an external power source for their operation. Active control on the other hand refers to systems which require a large power source to operate the actuators which supply the control forces whose magnitudes are determined using feedback from sensors that measure the excitation and/or the response of the structure. Semi-active control combines the features of active and passive systems. These systems require a small power source (e.g., a battery) to operate. They utilize the response of the structure to develop the control forces which are regulated by algorithms using the measured excitation and/or response.

Semi-active control systems include two categories: active variable stiffness and active variable damping. In the first category, the stiffness of the structure is adjusted to establish a non-resonant condition between the structure and excitation. Variable stiffness devices can be regulated to include or exclude the stiffness of a particular section of the structure such as the bracing system. In the second category, supplemental energy dissipation devices such as fluid, friction, and electrorheological dampers, are modified to allow adjustments in their mechanical properties to achieve most reductions in the response. In both categories, similar to passive systems, control forces are generated using the motion of the structure and like active systems, controllers are used to monitor feedbacks and develop the appropriate command signals for selecting the stiffness or the damping coefficient of the device.

This study focuses on the use of semi-active control algorithms for structures with variable damping devices. Several investigators have studied the suitability of variable dampers and have found them to be effective in reducing the response of structures to different dynamic loadings. In addition to requiring a small power source to operate, the control forces developed by these devices oppose the direction of motion; thereby, enhancing the overall stability of the structure.

The next section presents a brief summary of previous work on development of semi-active control algorithms for variable damping devices. Three algorithms are discussed and their effectiveness in reducing the displacement and acceleration responses of structures to seismic loading is examined. The algorithms are used in several structures modeled as single- and multi-degree-of-freedom systems subjected to different earthquake excitations to demonstrate their effectiveness in reducing the response.

**BLANK PAGE**

## 2. SUMMARY OF PREVIOUS WORK

For active variable dampers, the damping coefficient  $c(t)$  during the response can be adjusted between upper and lower limits,  $c_{max}$  and  $c_{min}$ ; i.e.,

$$c_{min} \leq c(t) \leq c_{max} \quad (2.1)$$

Several investigators have developed algorithms to select the proper damping coefficient during the response. Patten et al. (1993) and Sack et al. (1994) introduced a hydraulic actuator with an adjustable orifice and used a closed loop control algorithm to select the damping coefficient of the device at each increment of time. They used a "clipped optimal control algorithm" based on the linear quadratic regulator (LQR) with a check on the dissipation characteristics of the control force. Their results indicate that a variable damper can significantly reduce the response of a structure to seismic forces. In another study, Patten et al. (1994a) used a bang-bang (also referred to as two-stage, bi-state, or on-off) algorithm based on Lyapunov's method to select the damping coefficient. They used the algorithm for a 3-story frame and subjected the frame to the 1979 El Centro accelerogram. The variable damper reduced the response of the frame by approximately 54% when compared to the response with no control. Other studies have been carried out to investigate the effectiveness of similar devices in reducing the response of bridges to vehicle-induced vibrations (Patten et al., 1994b and 1996).

Feng and Shinozuka (1990, 1993) have shown that for isolated bridges, increasing the damping of the isolation system reduces the relative displacement but increases the absolute acceleration. They suggested that the isolation system should contain a variable damper and used two semi-active algorithms for regulating the damping coefficient of the device. One is a bang-bang algorithm where  $c(t)$  is set to  $c_{max}$  when the relative displacement response divided by a referenced displacement is greater than the absolute acceleration response divided by a referenced acceleration. For the opposite case,  $c(t)$  is set to  $c_{min}$ . The other is an instantaneous optimal algorithm introduced by Yang et al. (1987). Numerical results indicate reductions of approximately 41% in peak displacement and 22% in peak acceleration responses for the case where the bridge was subjected to the S00E component of El Centro, 1940. Kawashima and Unjoh (1993, 1994) used a displacement dependent damping model to select the damping coefficient of a variable fluid damper. Analytical results and shake table tests of a 30 m long bridge indicated reductions of 24% and 44% in displacement and acceleration responses, respectively. In a later study, Yang et al. (1994) used the sliding mode control theory to design an algorithm for the variable damper suggested by Kawashima (1993, 1994). The idea behind the sliding mode control theory is to drive and maintain the response trajectory into a sliding surface where the motion of the structure is stable. Numerical results indicate that further reductions in the seismic response of the bridge can be achieved using the sliding mode algorithm (Kawashima and Unjoh, 1993 and 1994).

Dowdell and Cherry (1994a, 1994b) used a bang-bang semi-active linear quadratic regulator (LQR) algorithm to control the slip forces in friction dampers. They computed the response of a single and a six degree-of-freedom structure to a band limited white noise excitation with and without semi-active friction dampers. The results showed significant reductions in the inter-story drifts of the structures. In another study, Yang and Lu (1994) introduced a multi-stage semi-active friction damper to reduce the seismic response of cable-stayed bridges and showed numerically the effectiveness of the damper. Loh and Ma (1994) used a bang-bang semi-active algorithm based on Lyapunov theory for a 3-story frame and showed that the effect of variable dampers on the response can be significant. Calise and Sweriduk (1994) used robust control

techniques for variable damping devices and demonstrated their effectiveness in reducing the response.

In an extensive analytical and experimental study, Symans and Constantinou (1995) developed and tested a two-stage and a variable semi-active fluid damper. For the two-stage damper, they used a base shear coefficient and a force transfer control algorithm, while for the variable damper, they employed a feedforward, a skyhook damping, a linear quadratic regulator (LQR), and a sliding mode control algorithm. Their study included a single- and a three-story frame under different seismic excitations. The results indicated that while variable dampers significantly reduced the response compared to the no control case, no reduction was observed when compared to the device acting as a passive damper with a damping coefficient  $c_{max}$ .

The study by Symans and Constantinou (1995) indicates that the use of semi-active dampers in structures is inefficient when compared to passive systems. Since their study was limited to a SDOF structure with a period of 0.36 s and a MDOF structure with a fundamental period of 0.56 s, the efficiency of the device for other periods merits further investigation. This study considers a broad range of periods for which semi-active control with variable dampers may be more efficient than passive dampers in reducing the response. In the next sections, three semi-active control algorithms are examined to determine the effectiveness of variable dampers in reducing the seismic response. A semi-active variable device with a damping coefficient between  $c_{min}$  and  $c_{max}$  and the same device acting as a passive damper with damping coefficients  $c_{min}$  and  $c_{max}$  are compared to assess the effectiveness of the system.

### 3. DISCUSSION AND ANALYSIS

Increased damping in structures allows the dissipation of a larger portion of the input energy and consequently, a further reduction in the response. The reduction, however, depends on the flexibility or rigidity of the structure. Feng and Shinozuka (1990, 1993) have reported that for isolated bridges, increased damping has opposite effects on the absolute acceleration of the girder and the relative displacement between the girder and the piers. A similar observation has been made by Sadek et al. (1996) who showed that for flexible structures (structures with periods longer than approximately 1.5 s), an increase in damping while further decreases the displacement response, it usually increases the acceleration response. Variable dampers where the damping coefficient can be adjusted between an upper and a lower limit may be effective in reducing both the relative displacement and absolute acceleration responses. Reducing the absolute acceleration response may be important in designing structures which house sensitive equipment such as hospitals, communication centers, computer and electronic rooms, etc. where the equipment may be damaged by large floor accelerations. Large accelerations may also cause discomfort to occupants.

To illustrate the influence of supplemental damping and structural period on the seismic response of structures, six single-degree-of-freedom structures with periods  $T = 0.2, 1.0, 1.5, 2.0, 2.5,$  and  $3.0$  s and a structural damping ratio  $\beta$  of 0.05 are used. Two supplemental passive dampers with damping ratios  $\xi$  equal to 0.05 and 0.40 were considered. The structures were subjected to the set of 20 horizontal components of accelerograms listed in Appendix A. These records include a range of earthquake magnitudes, epicentral distances, peak ground accelerations, and soil conditions. The relative displacement and absolute acceleration response ratios are computed as the ratio of the peak response of the structure with the supplemental damper to the peak response without the damper. The average response ratios for the twenty records for the six structures are shown in Table 3.1. The table shows that for structures with  $T < 1.5$  s (rigid structures), increasing the supplemental damping ratio from 0.05 to 0.40 decreases both the relative displacement and absolute acceleration; whereas for structures with  $T \geq 1.5$  s (flexible structures), increasing the supplemental damping ratio decreases the relative displacement but increases the absolute acceleration. Therefore, for flexible structures, reductions in both the displacement and acceleration responses may be possible with a variable damper than with a passive damper (fixed damping ratio), i.e. achieving a displacement response close to that obtained with  $\xi_{\max}$  and an acceleration response close to that obtained with  $\xi_{\min}$ . For rigid structures, however, the efficiency of using a variable over a passive damper is questionable. In the next section, three semi-active control algorithms are discussed and compared with each other in order to examine the effectiveness of variable dampers in reducing the displacement and acceleration responses of structures.



Table 3.1 Summary of the average response ratios for six SDOF structures with passive damping

damping ratio (1)	T=0.2 s (2)		T=1.0 s (3)		T=1.5 s (4)		T=2.0 s (5)		T=2.5 s (6)		T=3.0 s (7)	
	$x_{\max}$	$a_{\max}$	$x_{\max}$	$a_{\max}$	$x_{\max}$	$a_{\max}$	$x_{\max}$	$a_{\max}$	$x_{\max}$	$a_{\max}$	$x_{\max}$	$a_{\max}$
$\xi_{\min} = 0.05$	0.81	0.82	0.81	0.83	0.81	0.84	0.84	0.88	0.86	0.91	0.89	0.95
$\xi_{\max} = 0.40$	0.46	0.54	0.42	0.72	0.46	0.94	0.54	1.19	0.56	1.36	0.59	1.55

#### 4. SEMI-ACTIVE CONTROL ALGORITHMS

The governing differential equation of motion for an  $n$ -degree of freedom structure with mass matrix  $M$ , damping matrix  $C$ , and stiffness matrix  $K$  with  $m$  semi-active dampers subjected to ground acceleration  $\ddot{x}_g(t)$  is given by:

$$M\ddot{x}(t) + C\dot{x}(t) + Kx(t) = Du(t) - M1\ddot{x}_g(t) \quad (4.1)$$

where the  $n$ -dimensional vector  $x(t)$  represents the relative displacement, the  $m$ -dimensional vector  $u(t)$  the control forces generated by the dampers, and the  $n$ -dimensional vector  $1$  the unit vector. The matrix  $D$  (size  $n \times m$ ) defines the locations of the control forces generated by the dampers. Using the state-space representation, Equation (4.1) takes the form:

$$\dot{z}(t) = Az(t) + Bu(t) + H\ddot{x}_g(t) \quad (4.2)$$

where  $z(t) = [x^T(t), \dot{x}^T(t)]$  is a  $2n$ -dimensional state vector. The system matrix  $A$  and the matrices  $B$  and  $H$  are given in Soong (1990). Three semi-active control algorithms for regulating the damping coefficient of the variable dampers are considered in this study. They include: a) a semi-active linear quadratic regulator (LQR), b) a semi-active generalized LQR, and c) a semi-active displacement-acceleration domain.

##### 4.1 Semi-Active LQR Algorithm

This algorithm, referred to herein as SA-1, is the classical linear quadratic regulator which has been extensively used for active control (Soong, 1990, Yang et al., 1992) and for semi-active control (Patten et al, 1993, 1994a; Dowdell and Cherry, 1994a, 1994b; Symans and Constantinou, 1995) of structures. In this algorithm, the control force  $u(t)$  in Equation (4.1) is selected by minimizing the following quadratic expression for the cost function over the duration of the excitation (Soong, 1990):

$$J = \int_0^{t_f} [z^T(t)Qz(t) + u^T(t)Ru(t)]dt \quad (4.3)$$

where  $t_f$  is the duration of excitation, and  $Q$  (size  $2n \times 2n$ ) and  $R$  (size  $m \times m$ ) are positive semi-definite and positive definite weighting matrices, respectively. If the elements of  $Q$  are larger than those of  $R$ , reducing  $z(t)$  has priority over reducing  $u(t)$ . For a closed-loop control configuration, minimizing Equation (4.3) subject to the constraint of Equation (4.2) results in a control force vector  $u(t)$  regulated only by the state vector  $z(t)$  such that:

$$u(t) = -\frac{1}{2}R^{-1}B^T Pz(t) = Gz(t) \quad (4.4)$$

where matrix  $G$  (size  $m \times 2n$ ) represents the gain matrix, and matrix  $P$  (size  $2n \times 2n$ ) is the solution of the classical Riccati equation which after neglecting the excitation term reduces to:

$$PA + A^T P - \frac{1}{2} P B R^{-1} B^T P + 2Q = 0 \quad (4.5)$$

The damping coefficient of damper  $i$  at time  $t$  can be computed from Equation (4.4) as

$$c_i^*(t) = \frac{u_i(t)}{\dot{x}_i(t)} = \frac{\sum_{j=1}^{2n} G_{i,j} z_j(t)}{\dot{x}_i(t)}, \quad i=1, m \quad (4.6)$$

where  $\dot{x}_i(t)$  is the relative velocity between the ends of damper  $i$ . Using the constraints in Equation (2.1), the damping coefficient is selected as

$$c_i(t) = \begin{cases} c_{\min,i} & c_i^*(t) \leq c_{\min,i} \\ c_i^*(t) & c_{\min,i} < c_i^*(t) < c_{\max,i} \\ c_{\max,i} & c_i^*(t) \geq c_{\max,i} \end{cases} \quad (4.7)$$

It can be shown that a passive damper with coefficient  $c_{\min}$  is obtained when  $Q$  in Equations (4.3) and (4.5) is a null matrix and a passive damper with coefficient  $c_{\max}$  is obtained when the elements of  $Q$  approach infinity.

To examine the effectiveness of this algorithm, two SDOF structures with periods  $T = 0.2$  s and 3.0 s and a structural damping ratio  $\beta = 0.05$  are considered. Each structure contains a variable damper with a damping ratio ranging from  $\xi_{\min} = 0.05$  to  $\xi_{\max} = 0.40$ . The structures are subjected to the 20 ground excitations listed in Appendix A. In the analysis,  $R$  is a scalar set equal to  $1/K$  and  $Q$  is selected as (see Wu et al., 1995)

$$Q = q \begin{bmatrix} K & 0 \\ 0 & M \end{bmatrix} \quad (4.8)$$

where  $q$  is a parameter reflecting the importance of the reduction in the state vector  $z(t)$  or the control force vector  $u(t)$ . The mean response ratios (the average of the peak displacement or acceleration response with semi-active control divided by their counterparts with no control) for  $q$  ranging from 0 to 1.0 are computed and plotted in Figure 4.1 for  $T = 0.2$  s and in Figure 4.2

for  $T = 3.0$  s. The plots indicate that for  $q = 0$ , the mean response ratios are very close to those with a passive damper with  $\xi_{\min} = 0.05$ , and for  $q \geq 0.5$ , the mean response ratios are nearly the same as those with a passive damper with  $\xi_{\max} = 0.40$  (compare columns 2 and 7 of Table 3.1 and the ordinates at  $q = 0$  and  $q = 1$  in Figures 4.1 and 4.2, respectively). For  $q$  between 0 to 0.5, the response ratios are between those with passive dampers with  $\xi_{\min}$  and  $\xi_{\max}$ . For the structure with  $T = 0.2$  s (Figure 4.1), increasing  $q$  decreases both the relative displacement and absolute acceleration. For the structure with  $T = 3.0$  s (Figure 4.2), however, increasing  $q$  decreases the relative displacement but increases the absolute acceleration. Figure 4.1 shows that for the structure with  $T = 0.2$  s, a variable damper is inefficient and the use of a passive damper with a damping ratio  $\xi_{\max}$  is more advantageous.

Shown in Table 4.1 (column 4) are the average response ratios for the structure with  $T = 3.0$  s where  $q$  is adjusted to give a displacement response ratio of 0.70 ( $q = 0.12$ ). This ratio is selected as a baseline for comparing the responses from the three algorithms. The table indicates that, compared with a passive damper with  $\xi_{\max}$  (column 3), using the SA-1 algorithm increases the relative displacement by 0.11 (11%)<sup>1</sup> and reduces the absolute accelerations by 0.40 (40%).

Table 4.1 Summary of the average response ratios for the structure ( $T = 3.0$  s) with passive and semi-active dampers

Control (1)	Passive, $\xi_{\min}$ (2)	Passive, $\xi_{\max}$ (3)	SA-1 (4)	SA-2 (5)	SA-3 (6)
$x_{\max}$	0.89	0.59	0.70	0.70	0.70
$a_{\max}$	0.95	1.55	1.15	0.95	1.09

## 4.2 Semi-Active Generalized LQR Algorithm

This algorithm, referred to herein as SA-2, was introduced by Yang et al. (1992) for active control of structures and is adopted for semi-active control in this study. In this algorithm, the cost function is augmented by imposing a penalty on the absolute acceleration of each degree-of-freedom to control the acceleration response of the structure. The generalized cost function has the form

$$J = \int_0^{t_f} [z^T(t)Qz(t) + \ddot{x}_a^T(t)Q_a\ddot{x}_a(t) + u^T(t)Ru(t)]dt \quad (4.9)$$

<sup>1</sup> The  $x_{\max}$  and  $a_{\max}$  in Table 2 are percentages of the uncontrolled response.

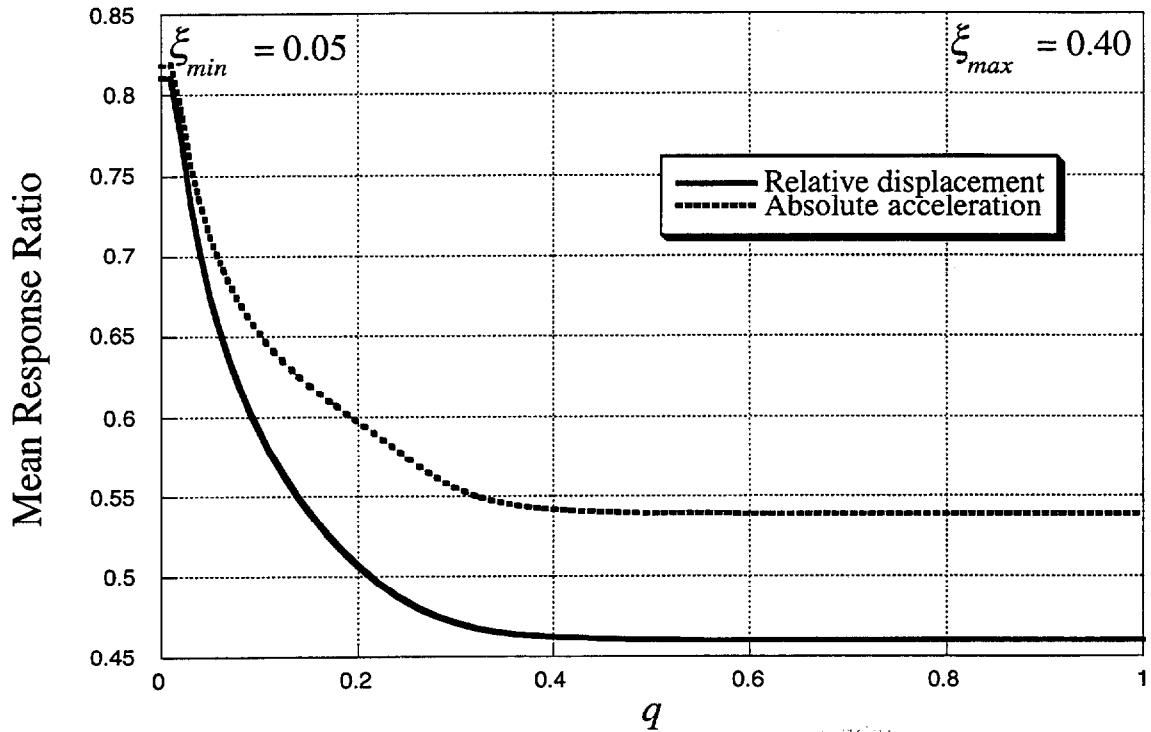


Figure 4.1 Variation of the displacement and acceleration response ratios with  $q$  for the SDOF structure with  $T = 0.2$  s using algorithm SA-1

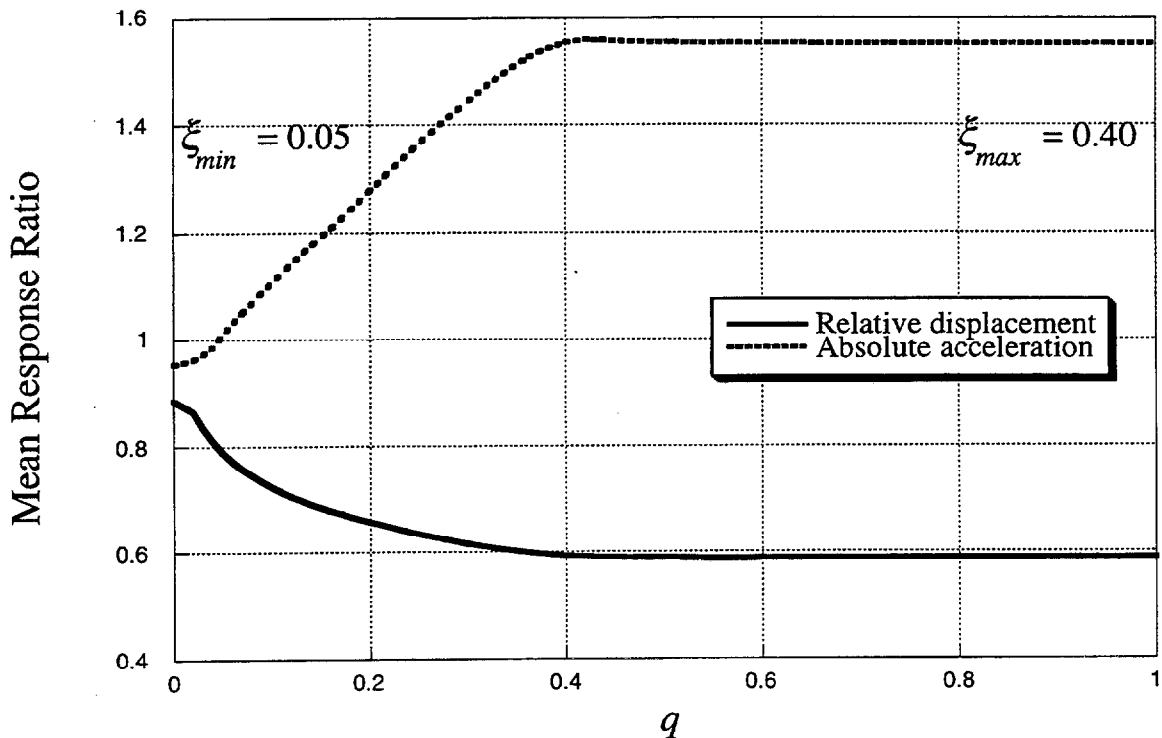


Figure 4.2 Variation of the displacement and acceleration response ratios with  $q$  for the SDOF structure with  $T = 3.0$  s using algorithm SA-1

in which  $\ddot{x}_a(t)$  is the absolute acceleration vector and  $Q_a$  (size  $n \times n$ ) is a symmetric positive semi-definite weighting matrix. If the elements of  $Q_a$  are larger than those of  $Q$ , reducing the absolute acceleration vector  $\ddot{x}_a(t)$  has priority over reducing the state vector  $z(t)$ . The absolute acceleration vector  $\ddot{x}_a(t)$  can be computed from Equation (4.1) as

$$\ddot{x}_a(t) = A_0 z(t) + B_0 u(t) \quad (4.10)$$

where  $A_0 = [-M^{-1}K, -M^{-1}C]$  and  $B_0 = M^{-1}D$ . The cost function, thus, takes the form

$$J = \int_0^{t_f} [z^T(t), u^T(t)] \begin{bmatrix} Q + A_0^T Q_a A_0 & A_0^T Q_a B_0 \\ B_0^T Q_a A_0 & R + B_0^T Q_a B_0 \end{bmatrix} \begin{bmatrix} z(t) \\ u(t) \end{bmatrix} dt \quad (4.11)$$

Minimizing Equation (4.11) subject to the constraint of Equation (4.2) results in a control force vector  $u(t)$  of the form

$$u(t) = -\frac{1}{2} \tilde{R}^{-1} (B^T \tilde{P} + 2B_0^T Q_a A_0) z(t) = \tilde{G} z(t) \quad (4.12)$$

where  $\tilde{G}$  (size  $m \times 2n$ ) is the gain matrix and  $\tilde{P}$  (size  $2n \times 2n$ ) is the solution to the classical Riccati equation which takes the form:

$$\tilde{P}\tilde{A} + \tilde{A}^T \tilde{P} - \frac{1}{2} \tilde{P} B \tilde{R}^{-1} B^T \tilde{P} + 2\tilde{Q} = 0 \quad (4.13)$$

in which

$$\begin{aligned} \tilde{R} &= R + B_0^T Q_a B_0 \\ \tilde{A} &= A - B \tilde{R}^{-1} B_0^T Q_a A_0 \\ \tilde{Q} &= Q + A_0^T Q_a A_0 - A_0^T Q_a B_0 \tilde{R}^{-1} B_0^T Q_a A_0 \end{aligned} \quad (4.14)$$

Similar to the SA-1 algorithm, the damping coefficient of damper  $i$  at time  $t$  can be expressed as

$$c_i^*(t) = \frac{u_i(t)}{\dot{x}_i(t)} = \frac{\sum_{j=1}^{2n} \tilde{G}_{i,j} z_j(t)}{\dot{x}_i(t)}, \quad i=1, m \quad (4.15)$$

where  $\dot{x}_i(t)$  is the relative velocity between the ends of damper  $i$ . Imposing the constraints in Equation (2.1), the damping coefficient will be

$$c_i(t) = \begin{cases} c_{\min,i} & c_i^*(t) \leq c_{\min,i} \\ c_i^*(t) & c_{\min,i} < c_i^*(t) < c_{\max,i} \\ c_{\max,i} & c_i^*(t) \geq c_{\max,i} \end{cases} \quad (4.16)$$

It can be shown that for a null  $Q_a$  matrix, the SA-2 algorithm reduces to the SA-1 algorithm.

The two SDOF structures with  $T = 0.2$  s and 3.0 s with a variable damper are analyzed using the SA-2 algorithm. The same scalar  $R = I/K$  and matrix  $Q$  (Equation 4.8) with  $q = 0.5$  for both  $T = 0.2$  s and  $T = 3.0$  s are used in this example. It should be noted that  $q = 0.5$  results in a response approximately the same as that using a passive damper with  $\xi_{\max} = 0.40$  (see Figures 4.1 and 4.2). For SDOF systems,  $Q_a$  is a scalar and equal to  $q_a$  which reflects the importance of the reduction in the state vector  $z(t)$  or the acceleration response vector  $\ddot{x}_a(t)$ .

The mean displacement and acceleration response ratios for the two SDOF structures subjected to the 20 accelerograms for  $q_a$  ranging from  $10^0$  to  $10^5$  for  $T = 0.2$  s and  $10^3$  to  $10^7$  for  $T = 3.0$  s are shown in Figures 4.3 and 4.4, respectively. The figures show that for small  $q_a$  the response with a variable damper is close to that with a passive damper with  $\xi_{\max} = 0.40$  (compare columns 2 and 7 of Table 3.1 and Figures 4.3 and 4.4, respectively). Figure 4.3 shows that for the structure with  $T = 0.2$  s, increasing  $q_a$  increases both the displacement and acceleration responses and again the variable damper is not as efficient as a passive damper with a damping ratio  $\xi_{\max} = 0.40$ . Figure 4.4 indicates that for the structure with  $T = 3.0$  s, the variable damper is effective in significantly reducing the acceleration response while slightly increasing the displacement response.

Shown in Table 4.1 (column 5) are the mean response ratios for the structure with  $T = 3.0$  s where  $q_a$  is adjusted to give a mean displacement response ratio of 0.70 ( $q_a = 1.0 \times 10^5$ ). The table shows that compared with a passive damper with  $\xi_{\max} = 0.40$  (column 3), the SA-2 algorithm increases the relative displacement by 11%, but it decreases the absolute accelerations by 60% (the acceleration response is the same as that with a passive damper with  $\xi_{\min} = 0.05$ , see column 2 of Table 4.1). This demonstrates the effectiveness of the SA-2 algorithm in reducing the acceleration response.

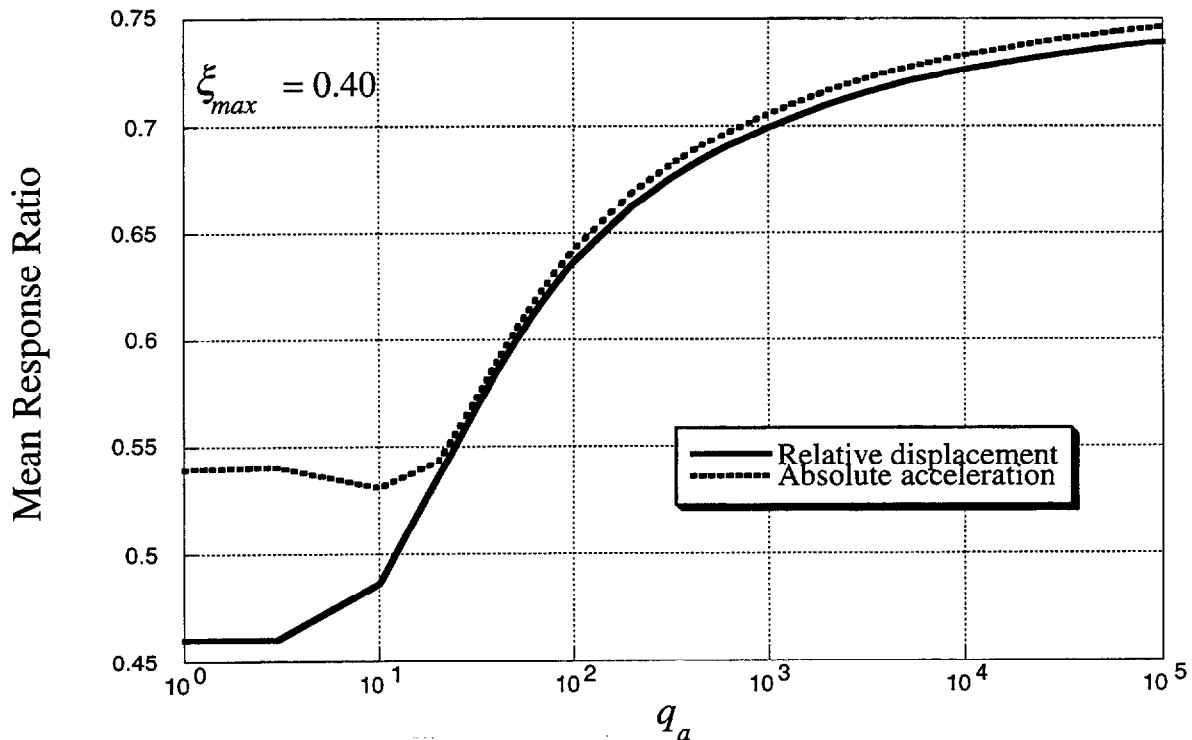


Figure 4.3 Variation of the displacement and acceleration response ratios with  $q_a$  for the SDOF structure with  $T = 0.2$  s using algorithm SA-2

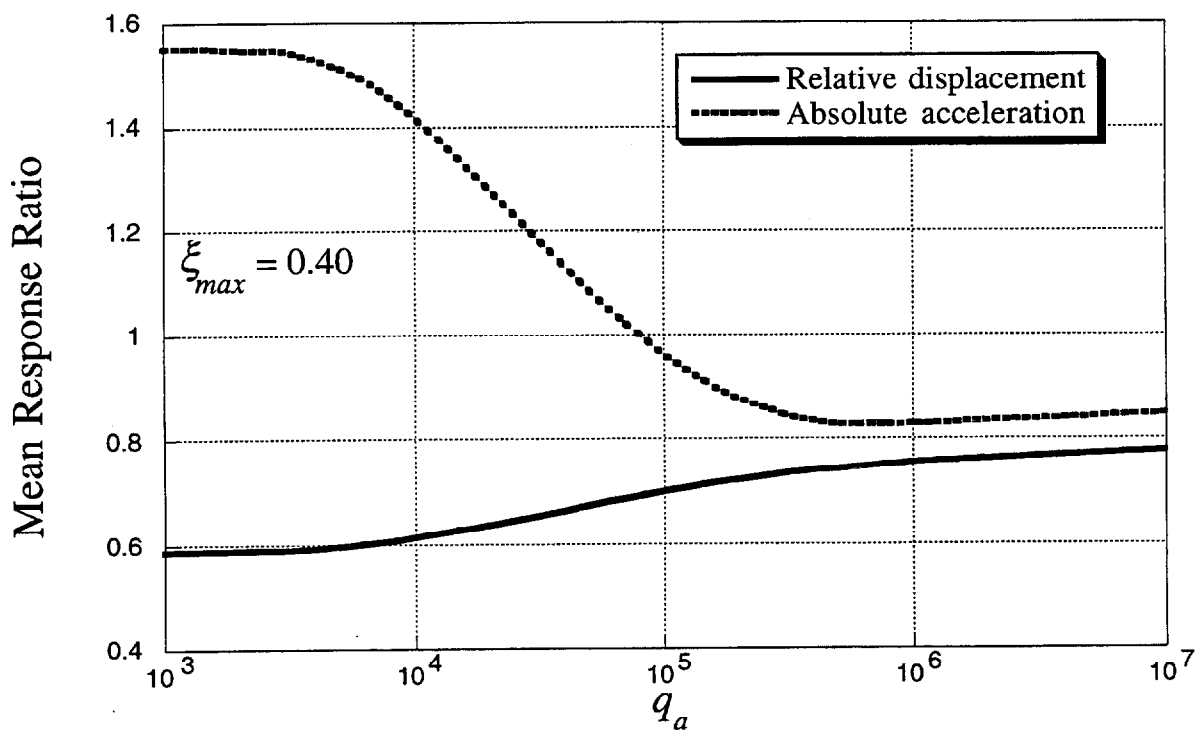


Figure 4.4 Variation of the displacement and acceleration response ratios with  $q_a$  for the SDOF structure with  $T = 3.0$  s using algorithm SA-2



### 4.3 Semi-Active Displacement-Acceleration Domain Algorithm

This algorithm, referred to herein as SA-3, is a refinement of the bang-bang algorithm presented by Feng and Shinozuka (1990, 1993). The refinement assumes a displacement-acceleration domain (Figure 4.5) where the horizontal axis represents the relative displacement response and the vertical axis the absolute acceleration response normalized to a reference parameter  $\Omega$ . This parameter, which has the unit of  $s^{-2}$ , is used as a weighting factor to impose different penalties on the displacement and acceleration responses. At any time  $t$ , the response may be represented by a single point on the displacement-acceleration domain. The angle  $\theta(t)$  between the horizontal axis and the line connecting the origin to the response point, Figure 4.5, is used to select the damping coefficient. This angle is:

$$\theta(t) = \tan^{-1} \frac{|\ddot{x}_a(t)| / \Omega}{|x(t)|} \quad (4.17)$$

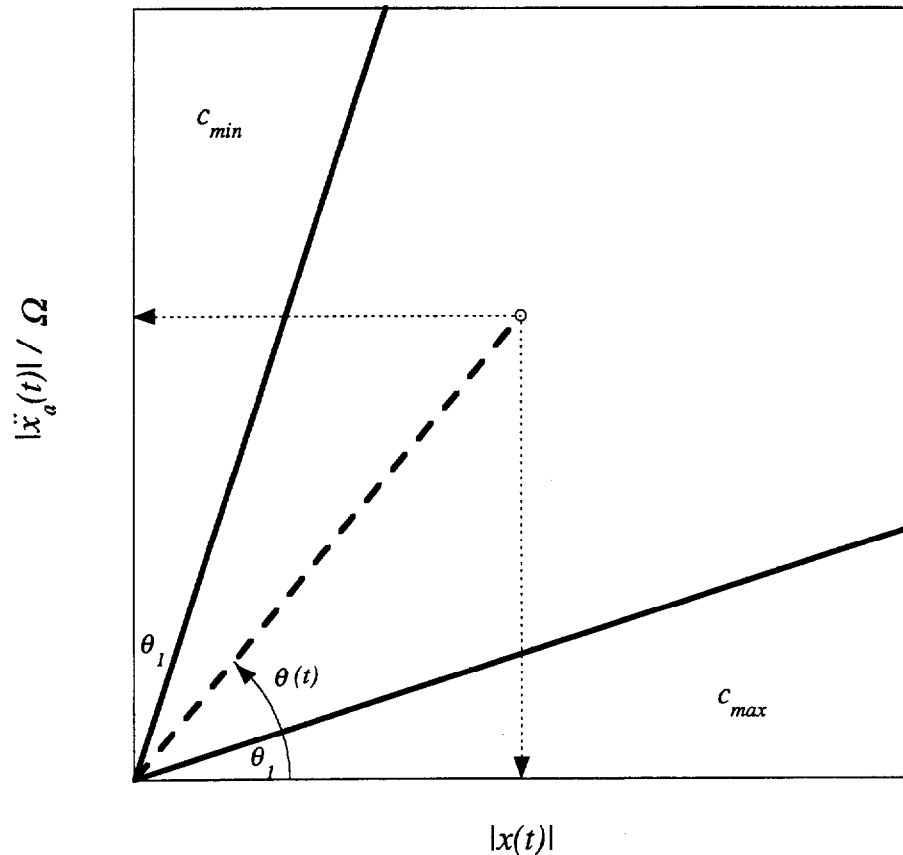


Figure 4.5 Displacement-acceleration Domain for algorithm SA-3

A small  $\theta(t)$  indicates a large displacement response with respect to the normalized acceleration and consequently requiring a higher damping coefficient. The opposite is true for a large  $\theta(t)$ . It is therefore desirable to assign a large damping coefficient  $c_{max}$  for small  $\theta$  ( $0 \leq \theta(t) \leq \theta_1$ ) and a small damping coefficient  $c_{min}$  for large  $\theta$  ( $\pi/2 - \theta_1 \leq \theta(t) \leq \pi/2$ ) where the angle  $\theta_1$  is yet to be determined. A linear variation of the damping coefficient with  $\theta(t)$  is used for  $\theta_1 \leq \theta(t) \leq \pi/2 - \theta_1$  (see Figure 4.5). Thus, the damping coefficient may be selected as follows:

$$c(t) = \begin{cases} c_{min} & \pi/2 - \theta_1 \leq \theta(t) \leq \pi/2 \\ c_{max} - \frac{c_{max} - c_{min}}{\frac{\pi}{2} - 2\theta_1} [\theta(t) - \theta_1] & \theta_1 < \theta(t) < \pi/2 - \theta_1 \\ c_{max} & 0 \leq \theta(t) \leq \theta_1 \end{cases} \quad (4.18)$$

It is seen from Equation (4.17) that increasing  $\Omega$  decreases  $\theta(t)$  which results in selecting a large  $c(t)$ . Consequently, reducing the relative displacement has priority over reducing the absolute acceleration. The opposite is true for decreasing  $\Omega$ . The reference parameter  $\Omega$ , therefore, reflects the importance of reduction in relative displacements or absolute accelerations.

Contrary to the first two algorithms (SA-1 and SA-2) which depend on the structural properties (stiffness, damping, and mass) which may be affected by errors in estimating their values, the SA-3 algorithm depends on the measured response only, Equations (4.17) and (4.18). The SA-3 algorithm is, therefore, robust with respect to the uncertainties in estimating the structural parameters.

The two SDOF structures with  $T = 0.2$  s and 3.0 s with variable dampers are analyzed using the SA-3 algorithm. Different values for  $\theta_1$  were assumed. It was found that a  $\theta_1$  between  $\pi/10$  to  $\pi/30$  resulted in the largest reductions in the response. The mean displacement and acceleration response ratios for the 20 records for  $\theta_1 = \pi/10$  and for  $\Omega$  ranging from  $10^1$  to  $10^5$  for  $T = 0.2$  s and  $10^2$  to  $10^4$  for  $T = 3.0$  s are plotted in Figures 4.6 and 4.7, respectively. The figures show that for small  $\Omega$ s, the response is approximately the same as that with a passive damper with  $\xi_{min} = 0.05$  and for large  $\Omega$ s, the response is nearly the same as that with a passive damper with  $\xi_{max} = 0.40$  (compare columns 2 and 7 of Table 3.1 and Figures 4.6 and 4.7, respectively). Figure 4.6 shows that for the structure with  $T = 0.2$  s, a semi-active control is inefficient and that a passive damper with  $\xi_{max}$  is more advantageous.

Shown in Table 4.1 (column 6) are the mean response ratios for the structure with  $T = 3.0$  s where the value of  $\Omega$  is adjusted to give a mean displacement response ratio of 0.70 ( $\Omega = 8$  s<sup>-2</sup>). The table indicates that compared with a passive damper with  $\xi_{max}$ , the SA-3 algorithm increases the relative displacement by 11% and reduces the absolute accelerations by 46%.

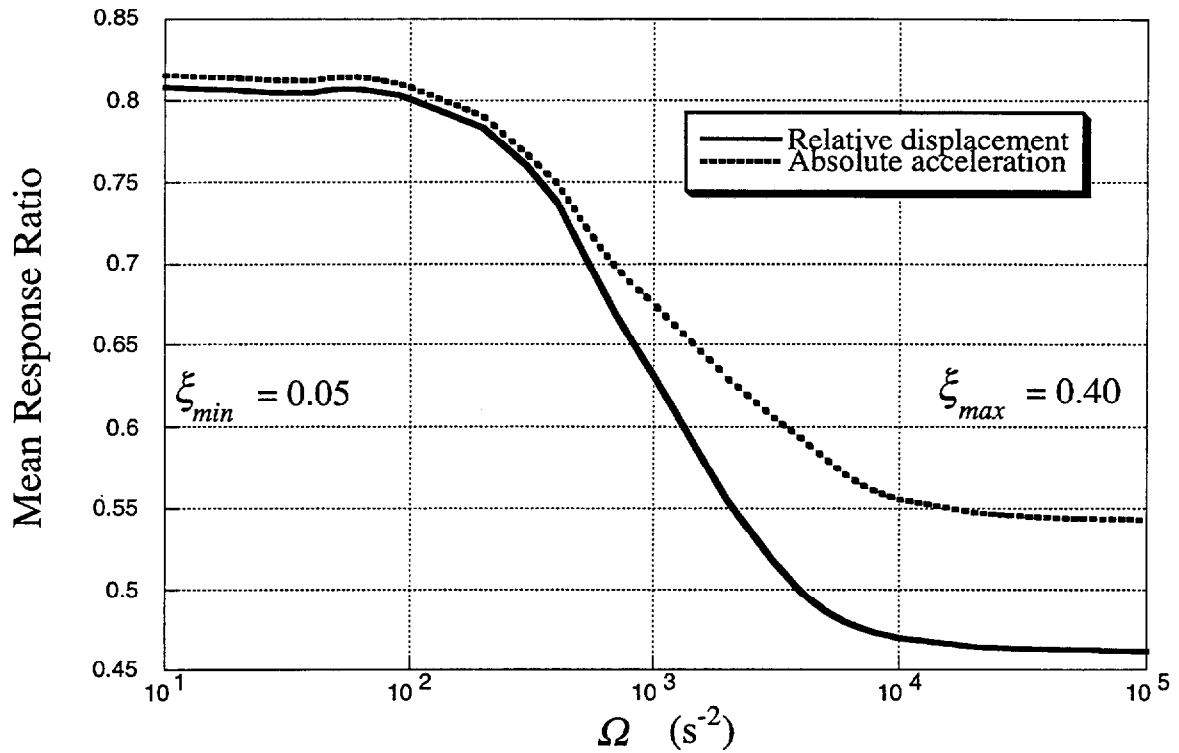


Figure 4.6 Variation of the displacement and acceleration response ratios with  $\Omega$  for the SDOF structure with  $T = 0.2$  s using algorithm SA-3

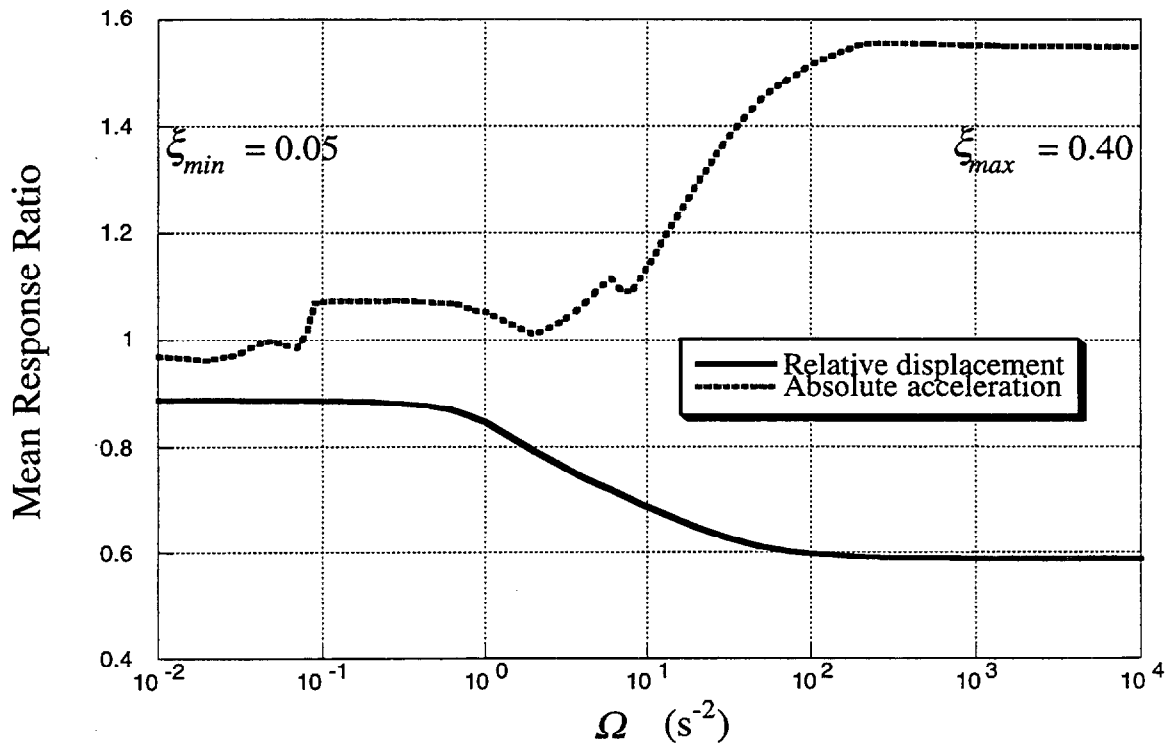


Figure 4.7 Variation of the displacement and acceleration response ratios with  $\Omega$  for the SDOF structure with  $T = 3.0$  s using algorithm SA-3

#### 4.4 Discussion and Comparisons of Algorithms

Based on the analyses and the results presented, the following may be concluded:

1. Variable dampers are more effective than passive dampers in reducing the seismic response of flexible structures ( $T \geq 1.5$  s) where increased damping has opposite effects on the displacement and acceleration responses. Examples of this type of structures include base-isolated structures, tall buildings, and isolated and cable-stayed bridges. For rigid structures ( $T < 1.5$  s), however, variable dampers are not effective in improving the response as compared to passive dampers.
2. Based on the results in Table 4.1, the generalized LQR algorithm (SA-2) is more effective than the other two in reducing the response. The use of the SA-2 algorithm results in an acceleration response nearly the same as that with a passive damper with a low damping ratio ( $\xi_{\min} = 0.05$ ) while the displacement response is increased by only 11% compared with a passive damper with a high damping ratio ( $\xi_{\max} = 0.40$ ). The effectiveness of the SA-2 algorithm results from the penalty imposed on controlling the absolute acceleration response which is a major concern in flexible structures with supplemental damping.
3. Both the SA-1 and the SA-3 algorithms result in similar responses, Table 4.1. The SA-3 algorithm, however, is somewhat preferable to SA-1 since it is inherently robust with respect to structural uncertainties.

**BLANK PAGE**

## 5. APPLICATIONS

Two examples are presented to demonstrate the performance of variable dampers in reducing the seismic response of structures. The first is a bridge modeled as a single-degree-of-freedom and the second is a six-story base-isolated frame modeled as a multi-degree-of-freedom.

### 5.1 Bridge

A bridge modeled as a SDOF structure was used to assess the effectiveness of the algorithms in reducing the seismic response. The bridge is similar to that used by Feng and Shinozuka (1990, 1993). It has a mass of  $1.02 \times 10^6$  kg and a hybrid control system consisting of an isolator with a stiffness 3300 kN/m and a variable damper. The damping ratio for the bridge is assumed as 2% and the damping coefficient of the variable damper varies between  $c_{min} = 150$  kN.s/m and  $c_{max} = 1200$  kN.s/m. The bridge was subjected to four accelerograms -- the N21E component of Taft Lincoln School Tunnel, Wheeler Ridge earthquake, 1954; the S74W component of Pacoima Dam, San Fernando earthquake, 1971; the 0 degree component of the Corralitos Eureka Canyon Road accelerogram, the Loma Prieta earthquake, 1989; and the 90 degree component of the Arleta Nordhoff Avenue Fire Station accelerogram from the Northridge earthquake, 1994; each scaled to a peak ground acceleration of 1.0g. The results of the analyses with no control and with passive control (passive damper) with damping coefficients  $c_{min}$  and  $c_{max}$  are shown in Table 5.1 (columns 2-4) which indicate that an increase in damping decreases the relative displacements and increases the absolute accelerations.

The bridge was also analyzed with a variable damper using the three algorithms. For the SA-1 algorithm, the scalar  $R$  is set equal to  $1/K$  and the matrix  $Q$  is computed by Equation (4.8). By varying  $q$ , different combinations of displacement and acceleration are obtained. Shown in Table 5.1 (column 5) are the responses for  $q = 0.12$  where it is observed that  $x_{max}$  and  $a_{max}$  are between those obtained with  $c_{min}$  and  $c_{max}$ . The bridge was also analyzed using the SA-2 algorithm with  $q = 0.6$  ( $q = 0.6$  resulted in a response approximately the same as that using a passive damper with  $c_{max}$ ) and different values of  $q_a$ . The results for  $q_a = 3 \times 10^5$  are shown in Table 5.1 (column 6) where it is noted that the displacement responses are close to (or even lower than) those with  $c_{max}$  and the acceleration responses are close to those with  $c_{min}$ . The analysis with the SA-3 algorithm was carried out for  $\theta_1 = \pi/10$  and different  $\Omega$  values. The results presented in Table 5.1 (column 7) are for  $\Omega = 7 \text{ s}^{-2}$ . Similar to the SA-1 algorithm, the responses are between those with a low and a high damping coefficient. The results in Table 5.1 underscore the advantage of using the SA-2 algorithm.

### 5.2 Base-Isolated Frame

A six-story base-isolated frame was considered to examine the effectiveness of the three algorithms in reducing the displacement and acceleration responses of MDOF structure. The column stiffnesses are  $k_i = 3 \times 10^5$  kN/m, floor masses  $m_i = 1.0 \times 10^5$  kg, and the damping ratio is assumed to be 5% in each mode. The frame is supported at its base by an isolator with a linear stiffness  $k_b = 9,000$  kN/m, a mass  $m_b = 1.4 \times 10^5$  kg, and a variable damper with damping coefficients between  $c_{min} = 100$  kN.s/m and  $c_{max} = 900$  kN.s/m. Tables 5.2 and 5.3 show the responses with passive dampers to the S74W component of Pacoima Dam, San Fernando earthquake, 1971; and the N21E component of Taft Lincoln School Tunnel, Wheeler Ridge earthquake, 1954; both scaled to a peak ground acceleration of 1.0g. The tables indicate

(columns 2 and 3 in each table) that an increase in the damping coefficient of the isolator decreases the displacements and increases the accelerations.

The frame was also analyzed with a variable damper at the base using the three algorithms. For the SA-1 algorithm, the  $R$  matrix is a scalar and is set equal to 1, and the  $Q$  matrix is computed from Equation (4.8). Similar to the SDOF case, different displacement and acceleration responses are obtained by varying  $q$ . Column 4 in Tables 5.2 and 5.3 show the responses when  $q = 700$  where it is observed that the absolute accelerations are reduced and the displacements are increased when compared with the response with a passive damper with  $c_{max}$ .

For the analysis using the SA-2 algorithm, the scalar  $R = 1$  and the matrix  $Q$  with  $q = 5000$  which results in a response approximately equal to that with a passive damper with  $c_{max}$  are used. The  $Q_a$  matrix is selected as

$$Q_a = q_a I \quad (5.1)$$

where  $I$  is the identity matrix (size  $7 \times 7$ ). By varying  $q_a$  different penalties can be imposed on both the state and acceleration vectors. It was found that with  $q_a = 1.5 \times 10^5$ , a displacement close to that with a passive damper with  $c_{max}$  and an absolute acceleration close to that with  $c_{min}$  were obtained as shown in Tables 5.2 and 5.3 (column 5). To further reduce the acceleration response of the isolator, a higher penalty was imposed on its absolute acceleration by changing the element which corresponds to the isolator acceleration in the identity matrix -- element (7,7) -- to a larger number (7 instead of 1) and using a  $q_a = 10^5$ . This change resulted in a further reduction in the acceleration response of the frame as shown in Tables 5.2 and 5.3 (column 6).

A similar analysis was performed to investigate the effectiveness of SA-3 algorithm for the base-isolated MDOF structure where the displacement-acceleration domain was defined using the isolator response. The analysis (results are not included) showed that the algorithm was not effective and the accelerations obtained were greater than those using a passive damper with  $c_{max}$ .

Table 5.1 Summary of the response of the bridge with no control and with passive and semi-active dampers

Control (1)	No Control (2)		Passive, $c_{min}$ (3)		Passive, $c_{max}$ (4)		SA-1 (5)		SA-2 (6)		SA-3 (7)	
	$X_{max}$ $m$	$a_{max}$ $g$	$X_{max}$ $m$	$a_{max}$ $g$	$X_{max}$ $m$	$a_{max}$ $g$	$X_{max}$ $m$	$a_{max}$ $g$	$X_{max}$ $m$	$a_{max}$ $g$	$X_{max}$ $m$	$a_{max}$ $g$
Taft, 1954	0.250	0.083	0.236	0.085	0.181	0.137	0.199	0.122	0.175	0.079	0.197	0.125
Pacoima Dam, 1971	0.170	0.056	0.144	0.050	0.114	0.086	0.118	0.074	0.106	0.048	0.116	0.074
Corralitos, 1989	0.297	0.098	0.246	0.083	0.157	0.137	0.183	0.107	0.151	0.088	0.182	0.091
Arleta, 1994	0.488	0.161	0.411	0.143	0.308	0.218	0.340	0.195	0.350	0.128	0.358	0.185

Table 5.2 Response of the six-story base-isolated frame to the Pacoima Dam accelerogram

Level (1)	Passive, $c_{min}$ (2)		Passive, $c_{max}$ (3)		SA-1 (4)		SA-2a (5)		SA-2b (6)	
	$X_{max}$ $m$	$a_{max}$ $g$	$X_{max}$ $m$	$a_{max}$ $g$	$X_{max}$ $m$	$a_{max}$ $g$	$X_{max}$ $m$	$a_{max}$ $g$	$X_{max}$ $m$	$a_{max}$ $g$
Top	0.150	0.256	0.115	0.302	0.136	0.282	0.115	0.266	0.116	0.242
5	0.150	0.245	0.115	0.279	0.136	0.263	0.115	0.246	0.116	0.230
4	0.149	0.226	0.114	0.258	0.135	0.238	0.114	0.227	0.115	0.226
3	0.147	0.203	0.114	0.213	0.134	0.213	0.113	0.198	0.114	0.204
2	0.145	0.208	0.112	0.223	0.132	0.212	0.112	0.211	0.112	0.200
1	0.143	0.212	0.111	0.245	0.130	0.224	0.110	0.224	0.110	0.210
Base	0.139	0.212	0.108	0.261	0.127	0.239	0.107	0.235	0.108	0.223



Table 5.3 Response of the six-story base-isolated frame to the Taft accelerogram

Level	Passive, $c_{min}$ (2)		Passive, $c_{max}$ (3)		SA-1 (4)		SA-2a (5)		SA-2b (6)	
	$X_{max}$ m	$a_{max}$ g	$X_{max}$ m	$a_{max}$ g	$X_{max}$ m	$a_{max}$ g	$X_{max}$ m	$a_{max}$ g	$X_{max}$ m	$a_{max}$ g
Top	0.170	0.337	0.141	0.428	0.161	0.370	0.134	0.378	0.136	0.396
5	0.169	0.311	0.140	0.392	0.160	0.340	0.133	0.370	0.135	0.374
4	0.167	0.273	0.138	0.322	0.158	0.286	0.132	0.324	0.134	0.336
3	0.164	0.278	0.135	0.326	0.155	0.305	0.129	0.319	0.132	0.333
2	0.161	0.308	0.132	0.392	0.151	0.357	0.127	0.345	0.129	0.346
1	0.157	0.334	0.128	0.432	0.147	0.384	0.124	0.362	0.127	0.343
Base	0.153	0.351	0.124	0.447	0.143	0.404	0.121	0.360	0.124	0.330

## 6. CONCLUSIONS

The overall objective of this study was to investigate the effectiveness of variable dampers in reducing the response of structures to earthquake loading. Three semi-active control algorithms are presented and compared. They include: 1) a linear quadratic regulator (LQR) algorithm referred to as (SA-1) which has been used extensively in active and semi-active control of structures; 2) a generalized LQR algorithm referred to as (SA-2) with a penalty imposed on the acceleration response which was introduced by Yang et al. (1992) for active control and is adopted for use as a semi-active control algorithm in this study; and 3) a displacement-acceleration domain algorithm referred to as (SA-3) where the damping coefficient is selected based on the location of the response parameters on the displacement-acceleration plane.

Two single-degree-of-freedom structures (a flexible and a rigid) were analyzed with the three algorithms using 20 accelerograms for the excitation. The results indicate that:

- a) variable dampers can be effective in reducing the acceleration response of flexible structures such as base-isolated and tall buildings, and isolated and cable-stayed bridges where an increase in damping adversely affects the acceleration response. Variable dampers, however, are not effective for rigid structures as compared to passive dampers;
- b) the SA-2 algorithm is more efficient than the other two in reducing the displacement and acceleration responses. The efficiency of this algorithm is, in most part, due to the penalty imposed in controlling the absolute acceleration response; and
- c) the SA-1 and SA-3 algorithms result in similar efficiency in reducing the response of single-degree-of-freedom structures, although the SA-3 Algorithm is more robust.

The three algorithms were used to compute the seismic response of an isolated bridge modeled as a SDOF structure and a base-isolated frame modeled as a MDOF structure. The results indicate that for these two structures which can be classified as flexible, variable dampers are quite effective in reducing the displacement and acceleration responses. The SA-3 algorithm, however, is not effective as the other two for multi-degree-of-freedom structures.

**BLANK PAGE**

## REFERENCES

1. Calise, A. J. and Sweriduk, G. D., (1994), "Active damping of building structures using robust control," *Proc. U.S. 5th Nat. Conf. Earthquake Engrg.*, pp. 1023-1032.
2. Dowdell D. J. and Cherry, S., (1994a), "Structural control using semi-active friction dampers," *Proc. 1st World Conf. on Structural Control*, Los Angeles, CA., pp. FA1/59-68.
3. Dowdell D. J. and Cherry, S., (1994b), "Semi-active friction dampers for seismic response control of structures," *Proc. U.S. 5th Nat. Conf. Earthquake Engrg.*, pp. 819-828.
4. Feng Q. and Shinozuka, M., (1990), "Use of a variable damper for hybrid control of bridge response under earthquake," *Proc. U.S. Nat. Workshop on Structural Control*, University of Southern California, Los Angeles, CA., pp. 107-112.
5. Feng, Q. and Shinozuka, M., (1993), "Control of seismic response of bridge structures using variable dampers," *J. Intelligent Material Systems and Structures*, Vol. 4, pp. 117-122.
6. Kawashima, K. and Unjoh, S., (1993), "Variable dampers and variable stiffness for seismic control of bridges," *Proc. Int. Workshop on Structural Control*, Honolulu, Hawaii, pp. 283- 297.
7. Kawashima, K., Unjoh, S., and Mukai, H., (1994), "Seismic response control of highway bridges by variable damper," *Proc. U.S. 5th Nat. Conf. Earthquake Engrg.*, pp. 829-838.
8. Loh, C. H. and Ma, M. J., (1994), "Active-damping or active-stiffness control for seismic excited buildings," *Proc. 1st World Conf. on Structural Control*, Los Angeles, CA., pp. TA2/11-20.
9. Patten, W. N., Sack, R. L., Yen, W., Mo, C., and Wu, H. C., (1993), "Seismic motion control using semi-active hydraulic force actuators," *Proc. ATC-17-1 Seminar on Seismic Isolation, Passive Energy Dissipation, and Active Control*, Applied Technology Council, Redwood City, CA., Vol. 2, pp. 727-736.
10. Patten, W. N., Kuo, C. C., He, Q., Liu, L., and Sack, R. L., (1994a), "Seismic structural control via hydraulic semi-active vibration dampers (SAVD)," *Proc. 1st World Conf. on Structural Control*, Los Angeles, CA., pp. FA2/83-89.
11. Patten, W. N., He, Q., Kuo, C. C., Liu, L., and Sack, R. L., (1994b), "Suppression of vehicle induced bridge vibration via hydraulic semi-active vibration dampers (SAVD)," *Proc. 1st World Conf. on Structural Control*, Los Angeles, CA., pp. FA1/30-38.
12. Patten, W. N., Sack, R. L., and He, Q., (1996), "Controlled semi-active hydraulic vibration absorber for bridges," *J. Struct. Engrg.*, ASCE, Vol. 122(2), pp. 187-192.
13. Sack, R. L., Kuo, C. C., Wu, H. C., Liu, L., and Patten, W. N., (1994), "Seismic motion control via semi-active hydraulic actuators," *Proc. U.S. 5th Nat. Conf. Earthquake Engrg.*, pp. 311-320.
14. Sadek, F., Mohraz, B., Taylor, A. W., and Chung, R. M., (1996), "Passive energy dissipation devices for seismic applications," *Report NISTIR 5923*, National Institute of Standards and Technology, Gaithersburg, MD.

15. Soong, T. T., (1990), *Active Structural Control: theory and practice*, John Wiley & Sons, Inc., New York, NY.
16. Symans, M. D. and Constantinou, M. C., (1995), "Development and experimental study of semi-active fluid damping devices for seismic protection of structures," *Report No. NCEER-95-0011*, State University of New York at Buffalo, NY.
17. Wu, Z., Soong, T. T., Gattuli, V., Lin R. C., (1995), "Nonlinear Control Algorithms for peak response reduction", *National Center for Earthquake Engineering Research, Technical report NCEER-95-0004*, Buffalo, NY.
18. Yang, C. and Lu, L. W., (1994), "Seismic response control of cable-stayed bridges by semi-active friction damping," *Proc. U.S. 5th Nat. Conf. Earthquake Engrg.*, pp. 911-920.
19. Yang, J. N., Akbarpour, A., and Ghaemmaghani, P., (1987), "New Optimal Control Algorithms for Structural Control," *J. Engrg. Mech.*, ASCE, 113(9), pp. 1369-1386.
20. Yang, J. N., Li, Z., and Vongchavalitkul, S., (1992), "A generalization of optimal control Theory: linear and nonlinear structures," *Report No. NCEER-92-0026*, State University of New York at Buffalo, NY.
21. Yang, J. N., Li, Z., Wu, J. C., and Kawashima, K., (1994), "Aseismic hybrid control of bridge structures," *Proc. U.S. 5th Nat. Conf. Earthquake Engrg.*, pp. 861-870.

**APPENDIX A. EARTHQUAKE RECORDS USED IN THE STATISTICAL STUDY**

Earthquake	Mag.	Station Name	Source Distance (km)	Comp.	Peak Accel. (g)
Northwest California 10/07/1951	5.8	Ferndale City Hall	56.3	S44W	0.104
				N46W	0.112
San Francisco 03/22/1957	5.3	San Francisco Golden Gate Park	11.2	N10E	0.083
				S80E	0.105
Helena Montana 10/31/1935	6.0	Helena, Montana Carrol College	6.2	S00W	0.146
				S90W	0.145
Parkfield, California 06/27/1966	5.6	Temblor, California # 2	59.6	N65W	0.269
				S25W	0.347
San Fernando 02/09/1971	6.4	Pacoima Dam	7.3	S16E	1.172
		250 E First Street Basement, Los Angeles	41.4	N36E N54W	0.100 0.125
Loma Prieta 10/17/1989	7.1	Corralitos - Eureka Canyon Road	7.0	90 deg. 0 deg.	0.478 0.630
		Capitola - Fire Station	9.0	90 deg. 0 deg.	0.398 0.472
Northridge 01/17/1994	6.7	Arleta Nordhoff Ave. - Fire Station	9.9	90 deg. 360 deg.	0.344 0.308
		Pacoima Dam - Down Stream	19.3	265 deg. 175 deg.	0.434 0.415

**BLANK PAGE**

## APPENDIX B. LIST OF SYMBOLS

$A$	system matrix
$a_{max}$	maximum absolute acceleration response
$B$	control force location matrix in state-space
$C$	damping matrix
$c_{max}$	maximum damping coefficient
$c_{min}$	minimum damping coefficient
$c(t)$	damping coefficient of the variable damper
$D$	control force location matrix
$G$	gain matrix
$g$	gravity acceleration
$H$	excitation location matrix in state-space
$I$	identity matrix
$J$	performance index
$K$	Stiffness matrix
$k_b$	isolator stiffness
$M$	mass matrix
$m$	number of dampers
$m_b$	isolator mass
$n$	number of degrees of freedom
$P$	Riccati matrix
$Q$	weighting matrix
$Q_a$	weighting matrix
$q$	parameter or multiplier
$q_a$	parameter or multiplier
$R$	weighting matrix
$T$	natural period
$t$	time
$t_f$	duration of excitation
$u$	control force vector
$x$	displacement vector
$\ddot{x}_a$	absolute acceleration response
$\ddot{x}_g$	ground acceleration
$x_{max}$	maximum relative displacement
$z$	state vector
$\theta(t)$	angle defining the response in the displacement-acceleration domain
$\xi_{max}$	maximum damping coefficient of variable dampers
$\xi_{min}$	minimum damping coefficient of variable dampers
$\Omega$	reference parameter